Review Article

Toxicology Research and Application

Toxicology Research and Application
Volume 2: 1–15

DOI: 10.1177/2397847318794859
journals.sagepub.com/home/tor
SAGE

Exposure to ambient particulate matter induces oxidative stress in lung and aorta in a size- and time-dependent manner in rats

OG Aztatzi-Aguilar[1,2], A Valdés-Arzate[3], Y Debray-García[3], ES Calderón-Aranda[3], M Uribe-Ramirez[3], L Acosta-Saavedra[3], ME Gonsebatt[4], JA Maciel-Ruiz[4], P Petrosyan[4], V Mugica-Alvarez[5], MC Gutiérrez-Ruiz[6], LE Gómez-Quiroz[6], A Osornio-Vargas[7], J Froines[8], MT Kleinman[9], and A De Vizcaya-Ruiz[3]

Abstract

Exposure to particulate matter (PM) has been implicated in oxidative stress (OxS) and inflammation as underlying mechanisms of lung damage and cardiovascular alterations. PM is a chemical mixture that can be subdivided according to their aerodynamic size into coarse (CP), fine (FP), and ultrafine (UFP) particulates. We investigated, in a rat model, the induction of OxS (protein oxidation and antioxidant response), carcinogen-DNA adduct formation, and inflammatory mediators in lung in response to different airborne particulate fractions, CP, FP, and UFP, after an acute and subchronic exposure. In addition, OxS was evaluated in the aorta to assess the effects beyond the lungs. Exposure to CP, FP, and UFP induced time- and size-dependent lung protein oxidation and DNA adduct formation. After acute and subchronic exposure, nuclear factor erythroid-2 (Nrf2) activation was observed in the lung, by electrophoretic mobility shift assay, and the induction of mRNA antioxidant enzymes in the FP and UFP groups, but not in the CP. Cytokine concentration of interleukin 1β, interleukin 6, and macrophage inflammatory protein-2 was significantly increased in bronchoalveolar lavage fluid after acute exposure to FP and UFP. Activation of Nrf2 and expression of mRNA antioxidant enzymes were observed only after the subchronic exposure to FP and UFP in the aorta. Our results indicate that FP and UFP were mainly accountable for the oxidant toxic effects in the lung; OxS is spread from the lung to the cardiovascular system. We conclude that the biological mechanisms associated with transient OxS and inflammation are particle size and time-dependent exposure resulting in acute lung injury, which later reaches the vascular system.

[1] Cátedras-CONACYT
[2] Instituto Nacional de Enfermedades Respiratorias Ismael Cosío Villegas, CDMX, Mexico
[3] Departamento de Toxicología, Centro de Investigación y de Estudios Avanzados del Instituto Politécnico Nacional. Av. Instituto Politécnico Nacional, CDMX, México
[4] Departamento de Medicina Genómica y Toxicología Ambiental, Instituto de Investigaciones Biomédicas, Universidad Nacional Autónoma de México, CDMX, México
[5] Área de Química Aplicada, Universidad Autónoma Metropolitana, CDMX, México
[6] Departamento Ciencias de la Salud, Universidad Autónoma Metropolitana, and Unidad de Medicina Traslacional UNAM/INCICH, Instituto de Investigaciones Biomédicas, CDMX, México
[7] Department of Pediatrics, University of Alberta, Edmonton, Alberta, Canada
[8] Center for Occupational and Environmental Health, School of Public Health, University of California Los Angeles, Los Angeles, CA, USA
[9] Department of Medicine, School of Medicine, University of California-Irvine, Irvine, CA, USA

Corresponding author:
A De Vizcaya-Ruiz, Departamento de Toxicología, Centro de Investigación y de Estudios Avanzados del Instituto Politécnico Nacional. Av. Instituto Politécnico Nacional 2508, 07760, México, DF, México.
Email: avizcaya@cinvestav.mx

Keywords
Particulate matter, nuclear factor erythroid-2, inflammation, oxidative stress, lung, aorta

Date received: 29 May 2018; accepted: 25 July 2018

Background

Atmospheric pollution is a worldwide public health concern; continuous exposure to high levels of particulate matter (PM) in ambient air has been associated with increased respiratory and cardiovascular adverse health effects.[1] The consequences of PM exposure on human health are suggested to depend on the particles' aerodynamic size and chemical composition. PM is a polydisperse, dynamically mixed conglomerate of chemicals in solid or liquid form, and is made up of complex aggregates of inorganic material (e.g. oxides of transition metals), salts (e.g. ammonium nitrate and sulfates), organic material (e.g. carbonaceous material and polycyclic aromatic hydrocarbons (PAHs)), and aerobiological material (e.g. endotoxin, pollen, proteins) with a carbonaceous core. PM can be subdivided into three main aerodynamic fraction size (diameter particle, dp), coarse (CP, dp 10 to $\geq$2.5 μm), fine (FP, dp $\leq$ 2.5 μm), and ultrafine (UFP, dp $\leq$ 0.1 μm) particulates, because the sources of CP, FP, and UFP are different and possess different physicochemical properties that can influence adverse health effects following exposure.[2,3]

In addition, the aerodynamic size dictates where PM can deposit along the respiratory tract. CP deposits effectively in the nasopharyngeal region, while FP and UFP are able to penetrate into the gas exchange region interacting with the alveolar epithelium, and UFP can translocate to systemic circulation after depositing along all airways, particularly from the alveolar sacs and olfactory epithelium.[4] Coarse particles are particles that are predominantly mechanically generated from natural sources, including geological material, suspended soil, brake and tire wear, resuspended road dust, and biological material from pollen and bacteria. FP and UFP production is dominated by anthropogenic combustion-related emissions and products of gas to particle conversion in the atmosphere.

Metal and organic particulate components elicit the formation of reactive oxygen species (ROS) with subsequent potential induction of oxidative stress (OxS). Moreover, PM can stimulate secondary ROS generated as part of an inflammatory response.[5–7] These prooxidant factors can change the cellular redox state, and various transcription factors, such as the nuclear factor erythroid-2 (Nrf2), which are activated to remove and neutralize ROS and mitigate their harmful effects.[8] The essential protective role of Nrf2 in the lung is activated in circumstances against oxidative environmental pollutants, therapeutic agents, allergens, and pathogens.[9–11] Nrf2 controls the transcription of cytoprotective genes by recognizing the DNA cis-regulatory element, the antioxidant response element (ARE), in specific gene promoters of antioxidant and detoxifying enzymes.[6,11] Among these genes, glutathione S-transferase (GST), heme oxygenase 1 (HO-1), and superoxide dismutase 2 (SOD2) are known to be involved in a survival response that counteracts OxS, thereby protecting cells from adverse biological outcomes.[12,13]

Nevertheless, when the protective response fails or is overwhelmed by excessive ROS production, a pro-inflammatory condition can result with various cytotoxic effects.[14] Nrf2 response is mediated by a redox sensitive thiol(ate), and NF-κB transcription factor, which is responsible for the expression of pro- and anti-inflammatory cytokines, chemokines, and adhesion molecules that can have local and systemic effects. PM inhalation can lead to the expression of several biological mediators that may be involved in particulate-induced inflammatory processes, which can impact not only the lung, but also other organs, either directly induced by PM or as a secondary effect.[15]

As previously mentioned, in addition to the local pulmonary damage that is induced by PM exposure when OxS and inflammation are activated, secondary systemic effects that alter the translocation of PM or PM-induced mediators from the alveoli into circulation have been hypothesized to cause direct toxic cardiovascular effects. PM exposure augments the development and progression of atherosclerosis by exerting detrimental effects on clotting, vascular tissue, and myocardium through the same cellular and molecular mechanisms of OxS and inflammation observed in PM-related lung toxicity.[16]

Furthermore, the inflammatory and OxS responses have been associated with the induction of DNA damage in lung tissue.[17] A large number of chemicals present on the different fractions of PM, especially traffic-related particulates, have genotoxic or mutagenic activities, which can result in DNA adduct formation.[18] The organic compounds and metals found on PM induce DNA adducts, which is related to not only the particle's chemical composition but also to the accompanying OxS and inflammation induced by the different particulate components.

It is possible that exposure to FP and UFP can be more hazardous to human health than exposure to CP.[19] UFP may have a greater potential to induce OxS than do FP and CP.[4,20,21] More attention has been paid to UFP toxicity because they are emitted mainly by combustion sources

and contain a higher content of redox-cycling organic chemicals than do CP and FP. Ultrafine particles can be deposited deep in the lungs or even translocate to the systemic circulation, inducing cardiovascular injury and impairing endothelium or cardiac muscle.[5,14,21]

Although CP and FP could be less toxic than UFP and epidemiological studies have shown that these particles are significantly associated with adverse health effects such as cardiopulmonary mortality and morbidity, they represent nearly all the mass of ambient PM. While it can be shown in the laboratory that the differences among particulate fractions determine the extent of biological responses such as OxS, inflammation, and DNA damage, it has not been possible to convincingly demonstrate this in population-based health studies. Part of the problem is that PM is extremely variable with respect to its spatial and temporal distribution. Consequently, there are few, if any, exposure metrics that can be used to carry out population-based health outcomes studies of UFP exposures. Nevertheless, it is important to understand the mechanisms by which CP, FP, and UFP cause adverse effects.

Therefore, in the present study, we used a particle concentrator system to simultaneously expose rodents to purified air, and different chemically sized aerosols: CP, FP, and UFP.[22] We investigated the effects of acute (3 days) and subchronic (8 weeks) exposures on OxS potential, induction of inflammatory cytokines, and DNA damage as a result of the presence of DNA adducts in lung tissue. Additionally, we measured the OxS responses induced by the inhalation of the different PM fractions, in their initial target tissue, the lung, and in the aorta, to compare the oxidative effects of PM for extrapulmonary target tissues. We measured protein oxidation and DNA adduct formation in the lung as biomarkers of lung damage. We assessed the Nrf2 recognition signals of the ARE sense sequence, the expression of antioxidant *HO-1*, *SOD2*, and *GST* genes as responders to OxS, and TNF-α, IL-1β, IL-6, and MIP-2 cytokines in bronchoalveolar lavage fluid (BALF) as indicators of inflammation. Additionally, to establish whether PM fraction exposure affects the vasculature, we evaluated the Nrf2 ARE activation and binding activity and the gene expression of antioxidant *HO-1*, *SOD2*, and *GST* in the aorta as a representative of a late onset systemic vasculature effect.

Methods

Experimental groups and exposure

Animal care and use were carried out according to the "Principles of Laboratory Animal Care" (NIH, USA) and Mexican guidelines (NOM-062-ZOO-1999). Animal handling and exposure was described in protocol ID 363-06, approved by the Internal Institutional Committee for the Use and Care of Laboratory Animals (Comité Interno para el Cuidado y Uso de los Animales de Laboratorio). Healthy 6-week-old male Sprague-Dawley rats (300–350 g at the end of the exposure of each group), $n = 6$ (per group), were obtained from Harlan Sprague-Dawley, Inc. (Mexico City, Mexico). During the whole of the experimental period, animals were maintained in a freestanding clean room with a changing station docking port (bioBubble®, Fort Collins, Colorado, USA). The rats were provided with ultrafiltered water and food *ad libitum* and maintained in a light: dark photoperiod of 12:12 h. Size-segregated exposure aerosols were provided using a versatile aerosol concentration system. The system was designed to support *in vivo* toxicity studies when coupled to exposure chambers.[19,20] These groups were simultaneously exposed in whole body chambers to enriched concentrated particulate atmospheres containing CP, FP, and UFP. Control group animals were exposed to filtered air (FA). Animals were exposed for 5 h/day for 3 days (acute exposure) and 5 h/day, 4 days/week for 8 weeks (subchronic exposure). Animals were euthanized by intraperitoneal injection of sodium pentobarbital (60 mg/kg). At necropsy, each animal trachea was cannulated to obtain BALF; four lavages per animal were performed with an isotonic saline solution and were later pooled and centrifuged at 1000 r/min. Supernatant and cell pellets were stored at -80°C until analyses. After BALF procedure, the thorax was opened, and lung and aorta were removed, snap frozen in liquid nitrogen, and stored at -80°C for further analysis.

PM concentration measurement and chemical composition determination

CP and FP concentrations in the whole body chambers were determined gravimetrically using 37-mm Teflon filters (PTFE 2-μm pore, Gelman Science, Ann Arbor, Michigan, USA) sampled from the PM and ambient air and chambers to estimate particle exposures. These data and the chemical composition of PM_{10} and $PM_{2.5}$ have been previously reported.[23]

Protein oxidation

Oxidative modification of proteins generates protein carbonyl groups, which can be used as an index of oxidation status of all proteins. Carbonyl groups were immunodetected using an OxiBlot™ Protein Oxidative Detection Kit S7150 (Chemicon International from Merck-Millipore, Darmstadt, Germany), according to the manufacturer's instructions. Briefly, 20 μg of lung lysates were derivatized with 2,4-dinitrophenyl hydrazine (DNPH) solution at room temperature (RT) for 15 min before stopping the reaction by adding a neutralizing solution. The DNPH-tagged proteins were then subjected to sodium dodecyl sulfate polyacrylamide gel electrophoresis (SDS-PAGE), transferred onto polyvinylidene difluoride (PVDF) membranes and subsequently blotted with an anti-dinitrophenyl group (DNP) antibody for detection. The protein-antibody complex signal was visualized using enhanced chemiluminescence (ECL)

Western blotting detection reagents (GE Healthcare, Buckinghamshire, UK). The bands were visualized by exposure to X-ray film and photo-documented (UVP EC3 imaging system, UVP Inc., USA).

DNA isolation and ^{32}P-postlabeling analysis of carcinogen-DNA adducts

Lungs were frozen in liquid nitrogen, pulverized, and resuspended in a solution of 20 mM Tris hydrochloride (HCl), pH 8.0, 250 mM sodium chloride (NaCl), 100 mM ethylenediaminetetraacetic acid (EDTA), and 0.5% SDS (Sigma-Aldrich, St Louis, Missouri, USA). Suspensions were RNase and proteinase K treated, and DNA was isolated by phenol–chloroform extraction. The DNA concentration was determined spectrophotometrically at 260 nm. DNA adducts were analyzed by the nuclease P1 enrichment version of the ^{32}P-postlabeling assay according to the protocol by Phillips and Arlt (2007),[24] a method that is reported to be broadly applicable to a range of adducts that have general characteristics of being bulky, aromatic, or hydrophobic, similar to those formed by PAHs or aromatic amines. The labeled carcinogen-DNA adducts were separated by thin layer chromatography on PEI-cellulose plates (Macherey-Nagel, Düren, Germany) using the following solvents: D1, 1M sodium phosphate, pH 6.0; D2, 3.6M lithium formate, 8.5M urea, pH 3.5; and D3, 0.8M lithium chloride, 0.5M Tris, 8.5M urea, pH 8.0. The plates were autoradiographed and the diagonal radioactive zone was cut out for Cerenkov counting. The results were expressed as DNA adducts/10^8 nucleotides.

Lung and aorta tissue cytoplasmic and nuclear protein extraction

Cytoplasmic protein extracts were prepared from lungs by lysing tissues with Igepal CA-630 (0.58%) in 10 mM Hepes pH 7.9, containing 10 mM potassium chloride, 0.1 mM EDTA, 0.1 mM ethylene glycol-bis(β-aminoethyl ether)-N,N,N′,N′-tetraacetic acid (EGTA), 1 mM dithiothreitol (DTT), and 0.5 mM phenylmethylsulfonyl fluoride (PMSF) (Sigma-Aldrich), and centrifuging at 13,000 $\times$ g for 15 min at 4°C. The supernatants were stored at −80°C for further analysis. Pelleted nuclei were resuspended in 20 mM Hepes pH 7.9, containing 0.4 mM NaCl, 1 mM EDTA, 1 mM EGTA, 1 mM DTT, and 1 mM PMSF (Sigma-Aldrich), after mixing continuously for 15 min at 4°C, the samples were centrifuged at 13,000 $\times$ g at 4°C for 5 min. Nuclear protein fractions were recovered and stored at −80°C for further analysis.

Cytoplasmic Nrf2 analysis by Western blot

Cytoplasmic proteins were obtained from the supernatants during the nuclear extraction procedure extraction. Cytosolic protein (60 µg) was denatured, fractionated by 10% SDS-PAGE, and transferred onto PVDF membranes (Invitrogen, Carlsbad, California, USA). After blocking nonspecific antibody binding, the membranes were blotted with an anti-Nrf2 antibody (sc-722; Santa Cruz Biotechnology, Santa Cruz, California, USA) and anti-β actin (sc-47778; Santa Cruz Biotechnology) in phosphate buffered saline (PBS) containing 0.1% Tween® 20 (PBS-T). The protein-antibody complex signal was visualized with a chemiluminescent reagent (ECL plus Western blotting detection system; Amersham Pharmacia Biotech Inc., Piscataway, New Jersey, USA), the bands were visualized by exposure to X-ray film, and then the films were documented to analyze band density. Anti-β actin was used as a loading control.

Electrophoretic mobility shift assay of Nrf2

Activation of Nrf2 was examined by electrophoretic mobility shift assay (EMSA) using a consensus oligonucleotide 5′-TTTTCTGCTGACTCAAGGTCCG-3′ (Promega, Madison, Wisconsin, USA). The probe was labeled by T4 polynucleotide kinase (USB, Cleveland, Ohio, USA) with [$\gamma-^{32}$P] adenosine triphosphate (ATP) (3000 Ci/mmol, MP Biomedical, Irving, California, USA) and purified using Bio-spin 30 chromatography columns (BioRad, Hercules, California, USA), the binding reaction mixture was made as described by Valdés-Arzate et al.[25] using 20 mg of protein from nuclear extracts, in 5 ml of incubation buffer (50 mM Tris-HCl, pH 7.5, 200 mM NaCl, 5 mM EDTA, 5 mM b-mercaptoethanol, and 20% glycerol) and 1 mg of poly(dI-dC). Complexes were separated on non-denaturing 6% polyacrylamide gels and were visualized by autoradiography. In competition experiments, 100-fold molar excess of non-labeled oligonucleotide was added to the reaction mix for 5 min before addition of the labeled probe. The protein concentration of the nuclear extracts was determined by the Bradford method.[26]

Total lung and aorta RNA isolation and reverse transcriptase-polymerase chain reaction

Total RNA was isolated from lung and aorta with TRIzol reagent (Invitrogen™, Life Technologies, Thermo Fisher Scientific, Carlsbad, California, USA) following the reagent specifications. Total RNA (1 µg) was reverse transcribed into cDNA according to the manufacturer's instructions (SuperScript II, Invitrogen™, Life Technologies, Thermo Fisher Scientific). PCR amplifications were performed with cDNA by using 10 pM of gene-specific forward and reverse primers in an Applied Biosystems 2720 thermal cycler (PerkinElmer Applied Biosystems, Foster City, California, USA). PCR reactions products were electrophoresed on 1.5% agarose gel and stained with ethidium bromide. The intensity of each gene PCR product band was quantitated and normalized to the corresponding housekeeping GADPH or β-actin cDNA band intensity using VisionWorks®LS Analysis Software (UVP, Upland, California, USA). Primers used were as follows:

GADPH forward 5′-ACCACAGTCCATGCCATCAC-3′and reverse: 5′-GCCAGTGAGCTTCCCGTT-3′; β-actin forward 5′-CTATCGGCAATGAGCGGTTCC-3′ and reverse 5′-AGCACTGTGTTGGCATAGAGGTC-3′; HO-1 forward 5′-AGGGAAGGCTTTAAGCTGGTGATG-3′ and reverse 5′-CCTGCCAGTGGGGCCCATAC-3′; SOD2 forward 5-TCCCTATCTCTGTGGTGGTGATG-3′ and reverse 5′-TATCCTGGTCATAGCCGAAGTCTC-3′; GST forward 5′-GCTTCAAGGCTCGCTCAAGTC and reverse 5′-ATCATTCACCATATCCACCAAGGC-3′.

Cytokine measurement by enzyme-linked immunosorbent assay

The analyses of pro-inflammatory cytokines (IL-1β, TNF-α, and IL-6) and chemokine MIP-2 present in BALF were carried out using sandwich enzyme-linked immunosorbent assay (ELISA) in microplates (Nunc, MaxiSorb, Sigma-Aldrich). Kits for ELISA from PreproTech, Princeton Business Park, USA, were used. Capture antibodies IL-1β (900-K91), TNF-α (900-K73), IL-6 (500-p73Bt), and MIP-2 (500-P75) (50 µl/well at 2 µl/ml) were incubated overnight at 4°C. Microplates were washed four times with PBS buffer (PBS 0.5% Tween® 20–WB; Santa Cruz Biotechnology). Nonspecific binding sites were blocked with 300 µl blocking solution (1% bovine serum albumin (BSA) in PBS) and the plates were incubated for 1 h at 37°C. Microplates were washed four times, standard dilutions of IL-6 and MIP-2 were prepared at the concentrations of 0, 0.25 to 10 ng/ml, and TNFα and IL-1β standard solutions were prepared at the concentrations of 0, 0.046 to 3 ng/ml. Fifty microliters of standard solutions and BALF samples were added to the microplates, incubated for 2 h at RT, and these were removed by four washes. Biotinconjugated detection antibodies (100 µl/well, 0.5 µg/ml) were added and incubated for 2 h at RT. The microplates were carefully rinsed four times and incubated with avidin-peroxidase conjugate (100 µl at a dilution of 1:2000). After incubation, the microplates were washed four times, 50 µl TMB (3,3′,5,5′-tetramethylbenzidine) substrate was added (Santa Cruz Biotechnology), and plates were incubated for 30 min at RT. The reaction was stopped adding 50 µl of sulfuric acid (2M). Optical density was measured at 450 nm using a Spectra MAX-plus^{384} multiplate reader (Molecular Devices, Inc., Sunnyvale, California, USA). Each sample was analyzed in triplicate and analyte concentrations were calculated from the linear portion of the generated standard curve.

Statistical analysis

Comparisons among groups were done by one-way analysis of variance followed by Bonferroni's post hoc comparisons or by the nonparametric Kruskal–Wallis test, followed by Dunn's test (when variances were not uniform). For protein oxidation, DNA adducts, and pro-inflammatory cytokines, a mean $\pm$ standard error of the mean was calculated. The p values <0.05 were considered statistically significant. Data analyses were performed using SigmaPlot, version 11 (Systat Software, Inc., Point Richmond, California, USA).

Results

Acute exposure to PM induces protein oxidative damage in the lung

OxS resulting from an imbalance between oxidants and antioxidants can affect macromolecules. OxS induction by exposure to the three PM fractions was evaluated by measuring lung protein oxidation. Acute exposure to concentrated CP, FP, and UFP, all induced significant ($p \leq 0.05$) lung protein oxidation, compared to the FA group (Figure 1(a)). In contrast, no oxidative damage to lung proteins was induced following subchronic exposure to the three PM fractions compared with the control group (Figure 1(b)). Our data suggest that the oxidative protein damage induced by short-term exposure in the lung was resolved and did not persist after repeated exposures to PM for an extended period.

Carcinogen-DNA adduct formation in the lung depends on the type of PM fraction

DNA adducts can originate from reactions with electrophilic species[27] because the rats were probably also exposed to low levels of adduct-forming compounds in their diet, caging, and other aspects of their environment. We analyzed the number of carcinogen-DNA adducts in the lung after acute and subchronic exposure to PM. Exposure to PM resulted in a significant increase in the carcinogen-DNA adducts in rat lung compared with the FA group (Figure 1(c) and (d)). As shown in Figure 1(c), after acute exposure to all PM fractions, the carcinogen-DNA adducts increased significantly (CP: 8.96 $\pm$ 1.43; FP: 10.83 $\pm$ 1.23; and UFP: 8.63 $\pm$ 0.45, per 10^8 nucleotides) compared with FA (1.68 $\pm$ 0.08 per 10^8 nucleotides). Similar results were observed only for the subchronic group exposed to UFP (Figure 2(d)), in which the number of carcinogen-DNA adducts in the UFP group was statistically significantly higher (12.80 $\pm$ 0.96 per 10^8 nucleotides) than that in the control group (5.56 $\pm$ 0.35 per 10^8 nucleotides).

Our results indicate that short-term exposure to CP, FP, and UFP can generate a number of carcinogen-DNA adducts. However, their presence and prevalence were greater in the subchronic exposure to UFP, possibly due to their chemical composition and because they have a greater contact surface area that could produce enough DNA adducts to be detected.[7,28] We observed differences in the formation of DNA adducts between control groups after acute and subchronic exposure, although they represent a stable basal level.

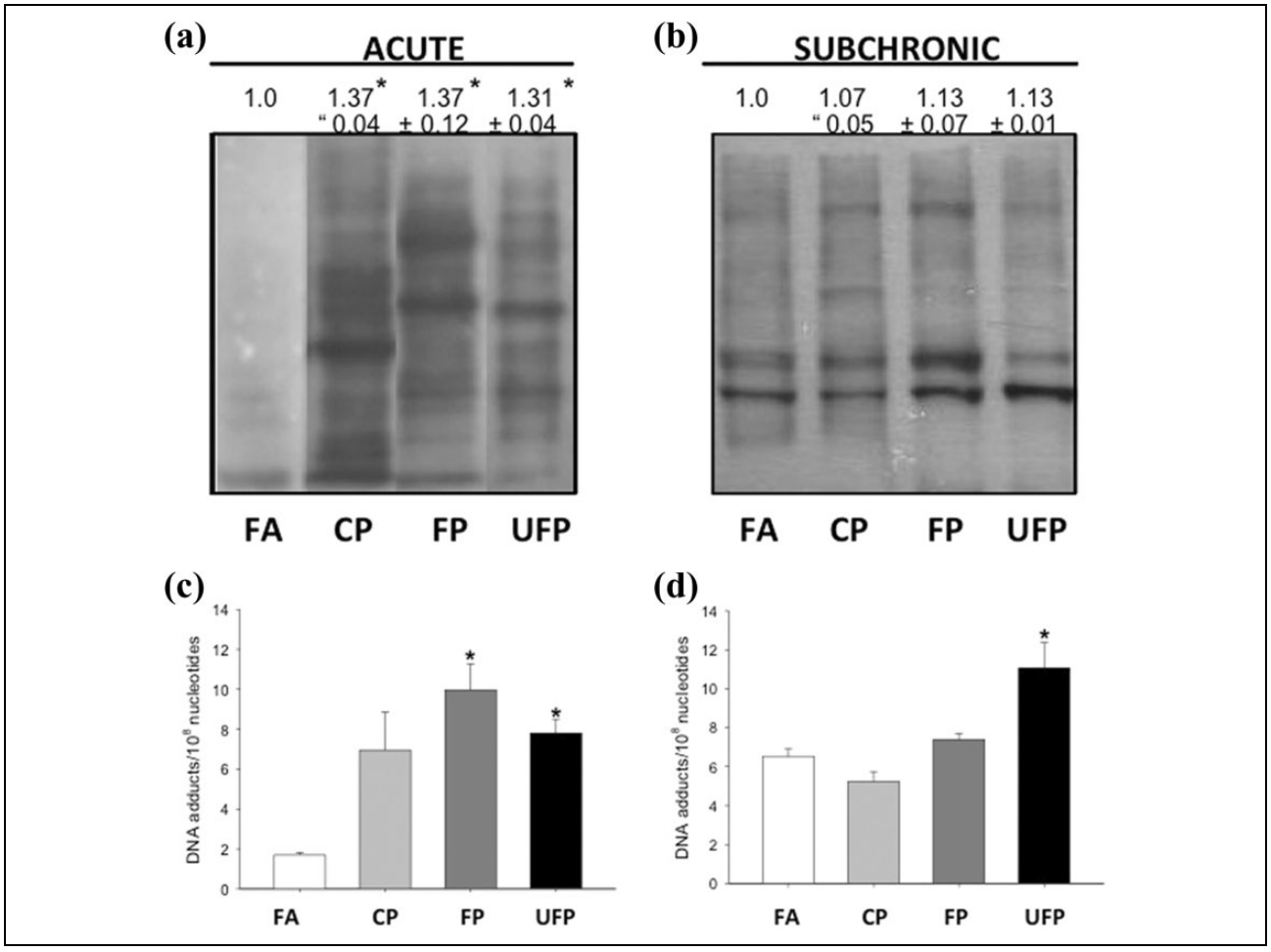

Figure 1. PM induced protein oxidation and DNA adducts in a time and particulate fraction dependent in lung tissue. Acute and subchronic exposure to FA, CP, FP, and UFP was performed. Protein oxidation in lung tissue, image representative of carbonyl detection from acute and subchronic exposure are showed in (a) and (b), respectively. PAH-DNA adducts in lung tissues from acute and subchronic exposure are showed in (c) and (d), respectively. Data are presented as mean ± SD ($n = 6$ rats/group). *indicates statistical differences ($p < 0.05$) respect to the FA group. PM: particulate matter; FA: filtered air; CP: coarse particulate; FP: fine particulate; UFP: ultrafine particulate; SD: standard deviation.

FP- and UFP-induced Nrf2-ARE binding activity in lung

Nrf2 nuclear translocation is triggered in response to OxS, and the nuclear accumulation of Nrf2 is considered as a marker of transcription factor activation, but in its constitutive state, Nrf2 is primarily localized in the cytosol.[11] We determined the presence of Nrf2 in cytosolic fractions following acute and subchronic exposure to PM, and using Western blot analyses with immunodetection cytosolic Nrf2 was decreased following both acute and subchronic FP and UFP exposure (Figure 2(a) and (c)), consistent with the premise that Nrf2 is activated and mobilized to the nucleus in response to FP and UFP exposure.

We examined the Nrf2–ARE binding activity by EMSA to confirm that in lung nuclear extracts the ARE binding activity was increased in the groups exposed to FP and UFP. As shown in Figure 2(b), acute exposure to FP and UFP increased the nuclear Nrf2–ARE binding activity (0.7- and 0.5-fold, respectively) compared with FA. Similar results were observed for subchronic exposure; Figure 2(d) shows the Nrf2–ARE activity in the lung of FP and UFP-exposed rats (0.6- and 1.0-fold, respectively). These results indicate that Nrf2 plays an important role in the cellular responses to FP and UFP exposure but not in the response to CP. In addition, the data trend suggests that there might have been a cumulative effect of the chronic exposures.

Expression of genes related to Nrf2 activation in the lung

We explored the effect of Nrf2 activation on the expression of the well-known Nrf2 genes, *HO-1*, *SOD2*, and *GST*. The induced expression of these genes confirmed increased Nrf2 activation in the rat lung after acute exposure to FP and UFP but not after CP exposure (Figure 3). The exposure to UFP induced a significant increase in the expression

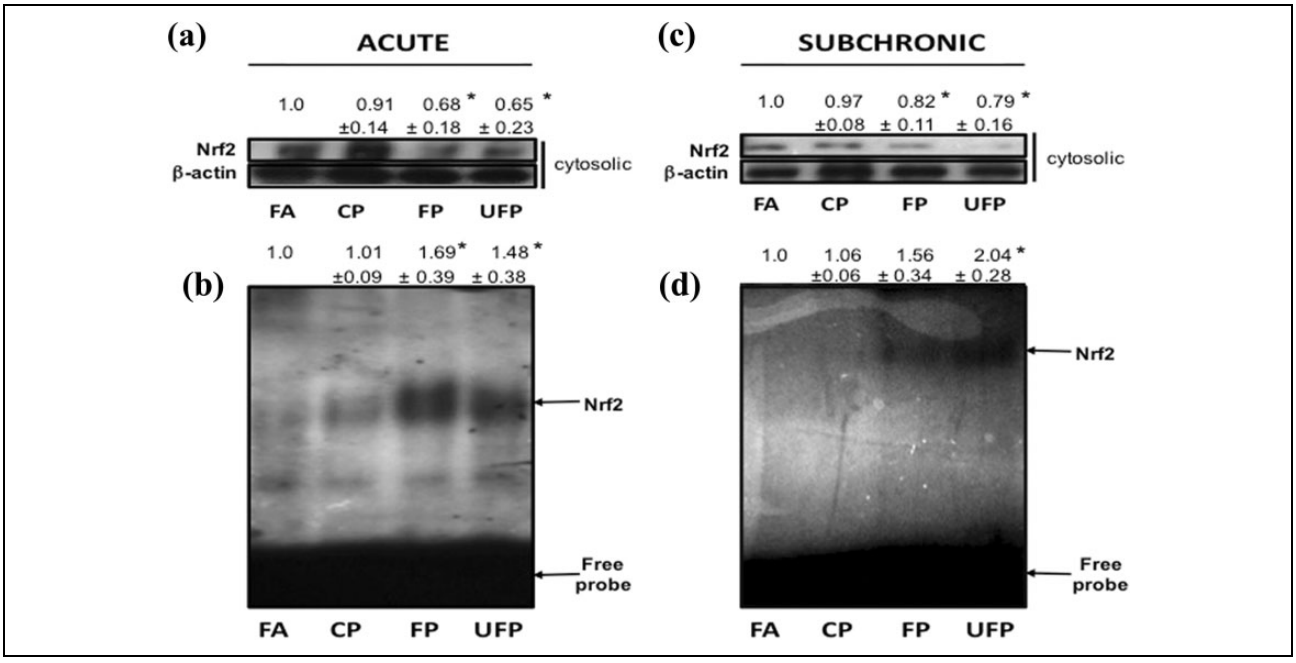

Figure 2. Nrf2 activation is size-dependent but not time-dependent in the lung. Nrf2 protein levels in the cytosolic extracts were detected by Western blot ((a) and (c)). Nuclear extracts were utilized for electrophoretic mobility shift assays of Nrf2 DNA binding activity ((b) and (d)). The upper arrow in the gel shift analysis indicates an Nrf2-DNA binding complex. Images are representative experiment of six animals per group of acute ((a) and (b)) and subchronic exposure ((c) and (d)) to FA, CP, FP, and UFP. Data in the top of images express as arbitrary densitometry units, we present the mean $\pm$ SD. *indicates statistical differences ($p < 0.05$) respect to the FA group. Nrf2: nuclear factor erythroid-2; FA: filtered air; CP: coarse particulate; FP: fine particulate; UFP: ultrafine particulate; SD: standard deviation.

of *HO-1* (0.54-fold; Figure 3(a)) and *SOD2* (1-fold; Figure 3(b)) compared with FA. UFP exposure did induce changes in the levels of GST mRNA (Figure 3(c)). FP exposure did not significantly change HO-1 mRNA (Figure 3(a)), but it did significantly increase *SOD2* expression (1.5-fold; Figure 3(b)) and increased the expression of *GST* (0.6-fold; Figure 3(c)), compared with the FA group.

Subchronic exposure to FP and UFP, but not CP, increased the expression of Nrf2-related genes compared to the FA group (Figure 3). HO-1 mRNA expression did not show changes in the exposure of all PM groups (Figure 3(d)). However, FP and UFP exposures significantly increased the expression of *SOD2* (0.6- and 1.5-fold, respectively; Figure 3(e)). Subchronic exposure to UFP also significantly increased the expression of *GST* (0.7-fold) with respect to the FA group (Figure 3(f)).

Acute exposure to FP and UFP induced the secretion of pro-inflammatory cytokines

We analyzed BALF from all experimental groups by ELISA. TNF-α, IL-1β, IL-6, and MIP-2 are mediators that initiate and propagate inflammatory responses.

The TNF-α concentration was slightly, but not significantly increased in BALF after acute and subchronic exposure to UFP, but not by the other PM fractions, compared to the FA group (Figure 4(a)). A significant increase in IL-1β was observed after acute exposure in BALF of the UFP group. After the subchronic exposure, the IL-1β concentration in all the exposed PM groups showed a tendency to decrease lower than the concentration level of the FA group, but it was not significant (Figure 4(b)). Acute exposure to FP and UFP significantly increased the BALF concentration of IL-6 and MIP-2 related to the FA-exposed group. Following subchronic exposure, no differences were observed (Figure 4(c) and (d)).

Aorta Nrf2 activation and antioxidant enzyme gene expression is time-dependent

We determined the cytosolic Nrf2 and DNA binding activity of Nrf2 in aortas of exposed and control rats as an index of OxS. No changes were observed after acute exposure (data not shown). However, after subchronic exposure to FP or UFP, the cytosolic Nrf2 decreased (Figure 5(a)), and EMSA analysis showed that the Nrf2 nuclear protein binding to the AREs increased significantly (1.33- and 1.48-fold, respectively) after subchronic exposure to FP and UFP compared with FA (Figure 5(a)), suggesting a molecular response against OxS generated by a subchronic exposure.

Based on Nrf2 nuclear activity, we did not observe changes in *HO-1*, *SOD2,* and *GST* gene expression from the FA group after acute exposure to all PM fractions (data

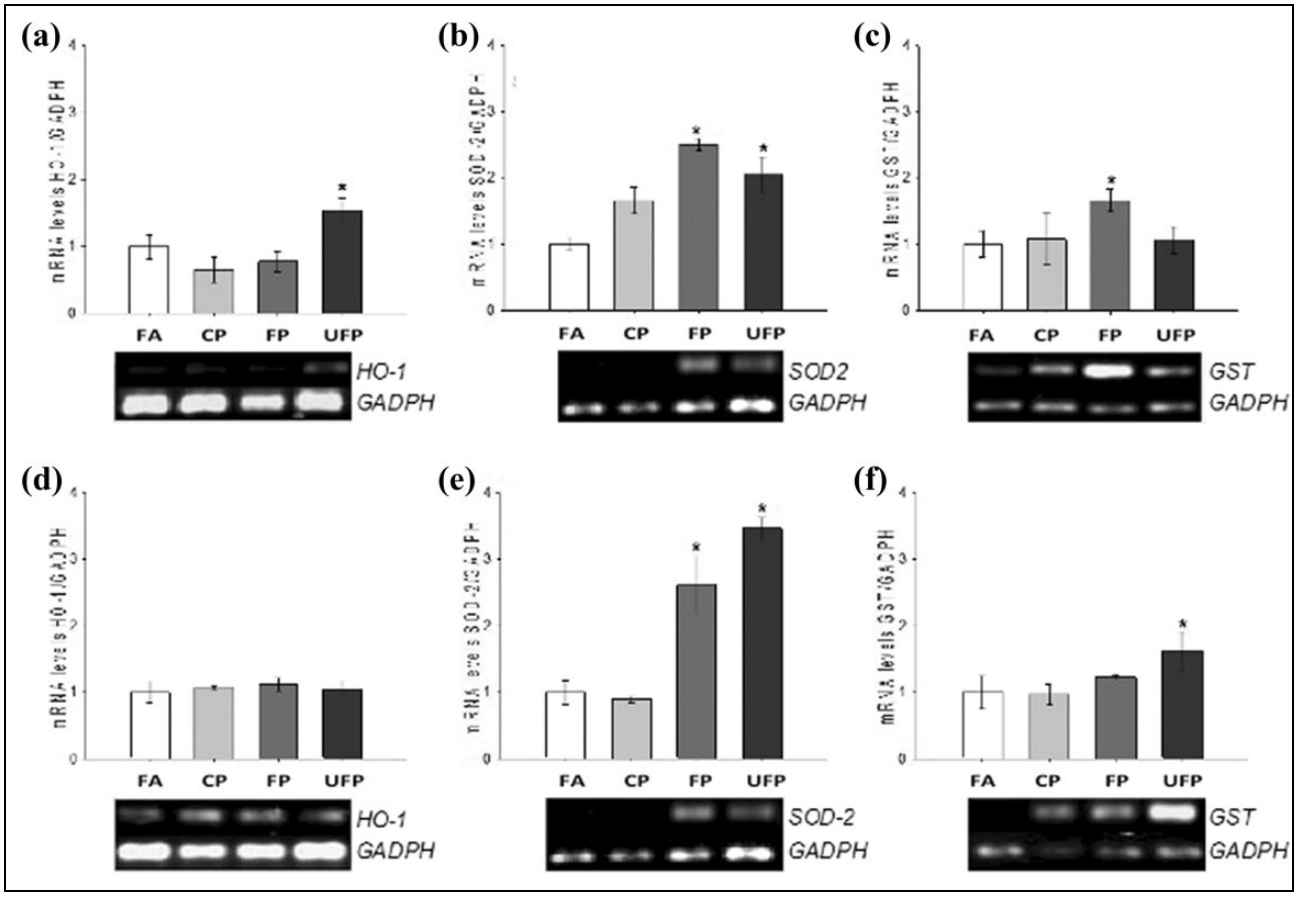

Figure 3. Antioxidant expression levels after acute and subchronic exposure are size-dependent in the lung. mRNA levels for HO-1, SOD2, and GST in the lung tissue were determined by RT-PCR for acute ((a), (b), and (c)) and subchronic ((d), (e), and (f)) exposure. Animals were exposed to FA as control group, CP, FP, and UFP. Bottom images in graphics represent one sample of at least six animals per group. Densitometry analysis was normalized with GADPH, and relative mRNA data are expressed as mean $\pm$ SD ($n = 6$ animals per group). *indicates statistical differences ($p < 0.05$) respect to the FA group. HO-1: heme oxygenase 1; SOD2: superoxide dismutase type-2; GST: glutathione S-transferase; RT-PCR: reverse transcriptase-polymerase chain reaction; FA: filtered air; CP: coarse particulate; FP: fine particulate; UFP: ultrafine particulate; SD: standard deviation; GADPH: glyceraldehyde-3-phosphate dehydrogenase.

not shown). The changes in *HO-1*, *SOD2*, and *GST* mRNA expression after the subchronic exposure to PM fractions were consistent with the nuclear Nrf2 activity (Figure 5(b) to (d)). The densitometric analysis demonstrated a statistically significant increase in *HO-1* mRNA expression in the CP- and UFP-exposed groups (2.37- and 3.69-fold, respectively) over the FA group (Figure 5(b)). *SOD2* mRNA expression in the aorta was observed in the FP and UFP groups, which exhibited a significant increase in the expression of *SOD2* (0.74- and 0.3-fold, respectively) compared with the FA group (Figure 5(c)). FP and UFP exposure displayed statistically significant increases in *GST* mRNA expression (0.71- and 0.67-fold, respectively) with respect to the FA group (Figure 5(d)).

Discussion

The results in this study suggest that (1) an initial local damage inducing inflammation and OxS in the lung mediates pathological effects in the aorta; and (2) this latter effect could be (a) due to the systemic translocation of FP and UFP to some of the chemical components or (b) secondary to mediators of OxS or inflammation.

Lung OxS and DNA damage

Exposure to PM has been associated with an increased occurrence of adverse cardiopulmonary effects in numerous epidemiological studies.[29] Nevertheless, there is still debate about which PM fraction and what components are responsible for the induction of the adverse effects. Accumulating evidence suggests that the pro-oxidative organic hydrocarbons (PAHs and quinones), and transition metals (copper, vanadium, chromium, nickel, cobalt, and iron) present in PM play a substantial role in ROS production and thus initiate an OxS process.[5,26,27]

OxS has been implicated in the etiology of several diseases linked to exposure to environmental toxicants, including PM, due to the increment of ROS concentrations that exceed antioxidant defenses and oxidase

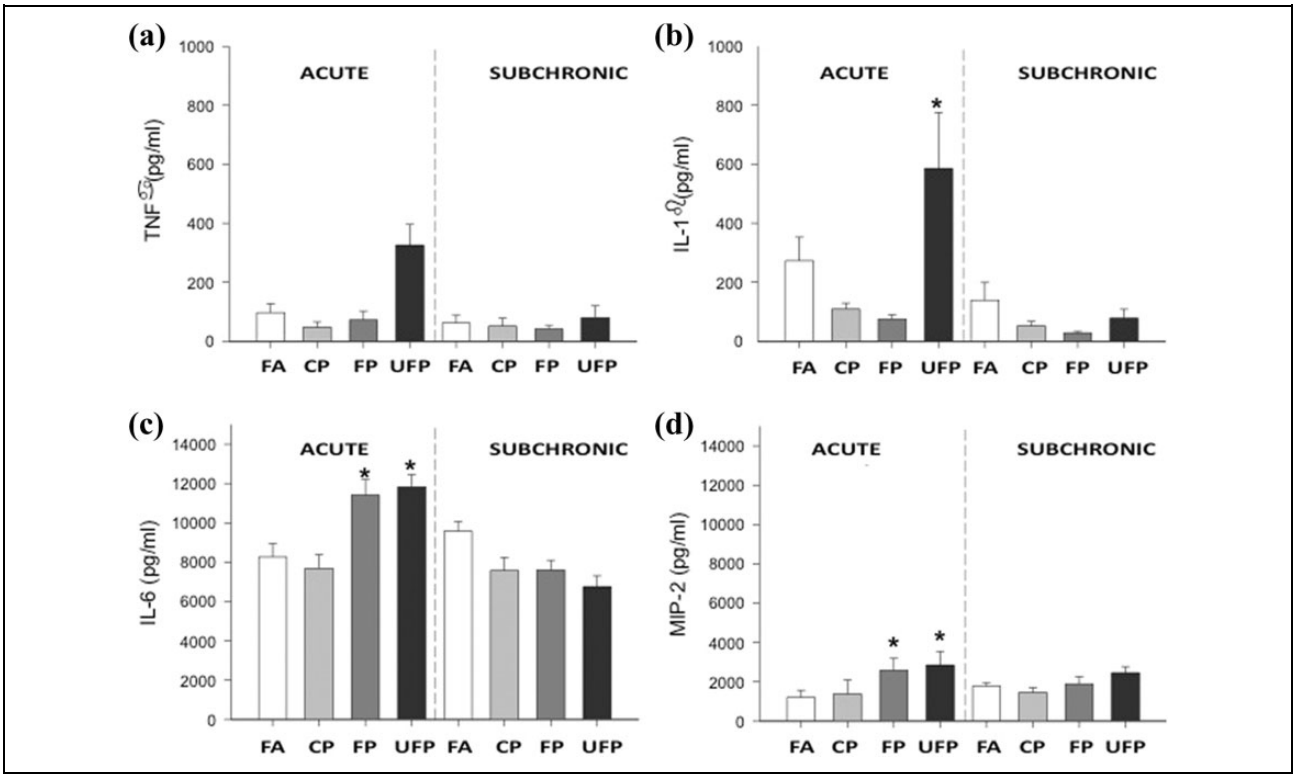

Figure 4. FP and UFP, but not CP fraction, increase acute inflammation. Cytokine protein levels in BALF from animals after acute and subchronic exposure to CP), FP, UFP, and FA as control group. Samples were analyzed by ELISA: (a) TNF-α, (b) IL-1β, (c) IL-6, and (d) MIP-2. Results are expressed as mean ± SEM ($n = 6$ animals/group). *indicates statistical differences ($p < 0.05$) respect to the FA group. FP: fine particulate; UFP: ultrafine particulate; CP: coarse particulate; BALF: bronchoalveolar lavage fluid; FA: filtered air; ELISA: enzyme-linked immunosorbent assay; TNF-α: tumor necrosis factor α; IL-1β: interleukin 1β; IL-6: interleukin 6; MIP-2: macrophage inflammatory protein-2; SEM: standard error of the mean.

macromolecules.[30–33] Protein carbonylation is an irreversible, nonenzymatic process that results in the introduction of carbonyl groups into the protein molecule, leading to changes in its conformation. Protein carbonylation has been associated with the development of cardiovascular and respiratory diseases[34,35] and has been used as a biomarker of oxidized proteins.[36] A significant increase in the number of oxidized proteins in the lung was detected following acute exposure to all PM fractions in this study, but protein oxidation was not observed in any of the groups exposed subchronically. This is perhaps consistent with upregulation of antioxidant defenses and elevated Nrf2 activation in the subchronic exposure. The OxS observed following acute exposure could be caused by organic compounds in PM, primarily in the FP and UFP fractions,[5] which cause extensive oxidative damage via the monooxygenase activity of cytochrome P450 and metal ions by Fenton reactions, contributing to the ROS concentrations.

We did not observe any protein oxidation after subchronic exposure to the three PM fractions studied. We propose that the observation of protein oxidation by PM fractions decrease after repeated exposure could be explained by (1) oxidized proteins that underwent proteasome degradation[37]; (2) the activation of an antioxidant response inducing the synthesis of nonenzymatic and enzymatic antioxidants[38]; and (3) the glutathionylation of proteins that protect them from oxidation.[39] These hypothesis need to be confirmed by further studies of subchronic and chronic exposure to PM.

OxS induced by PM exposure can contribute to carcinogen-DNA adduct formation as a result of its electrophilic chemical components. The number of carcinogen-DNA adducts increased in lung tissue after the acute exposure to all PM fractions, although, only statistically significant in the groups exposed to FP and UFP. The increase in the carcinogen-DNA adducts persisted after subchronic exposure. These data demonstrate that a short-term exposure to any PM fraction induced the formation of carcinogen-DNA adducts in exposed animals. However, after repeated exposure to CP and FP, the lung tissue was able to repair DNA adducts. Nevertheless, subchronic exposure to UFP induced similar adduct numbers with respect to the acute UFP exposure, probably reflecting differences in the reactivity and composition of UFP versus CP and FP.

It has been reported that the PAH content in PM contributes to the formation of DNA adducts.[14,36] In addition,

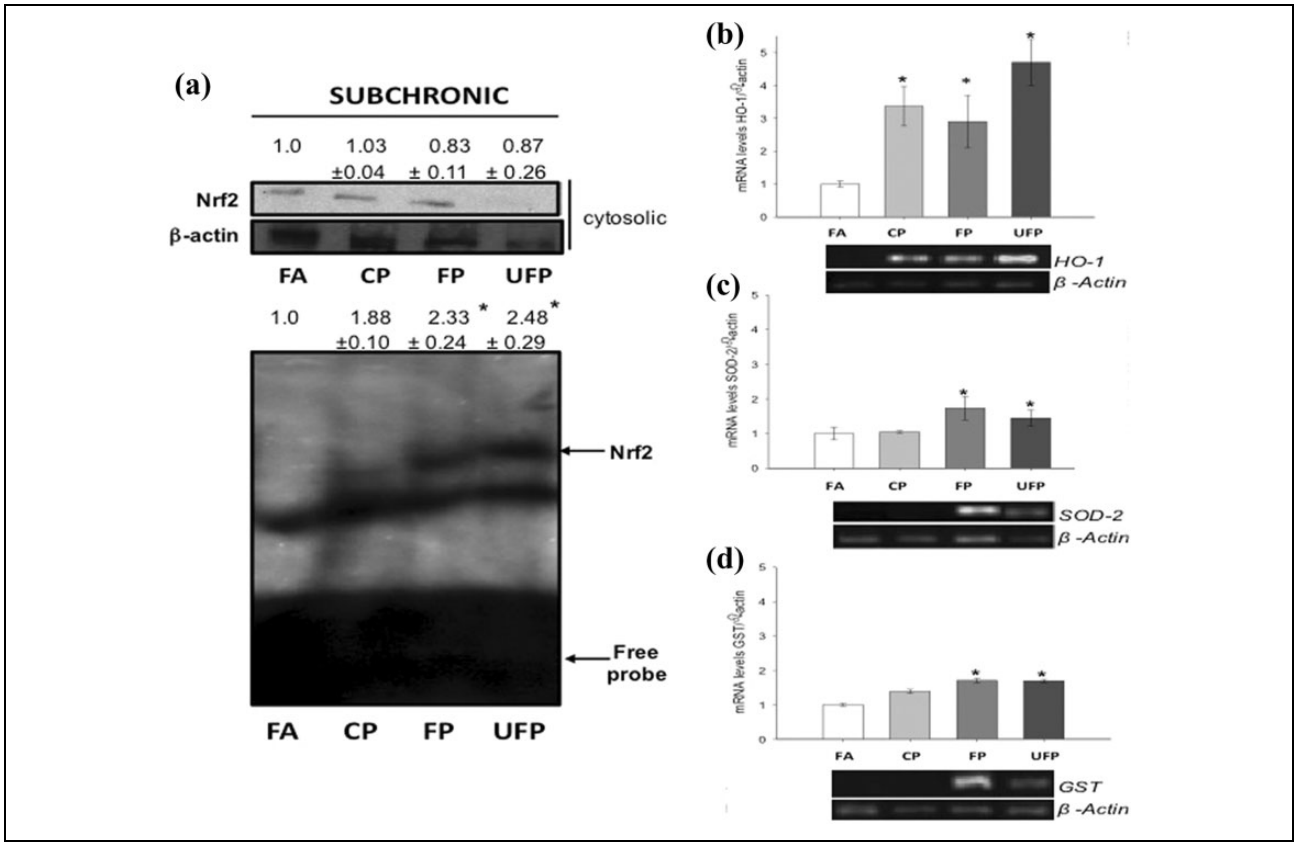

Figure 5. FP and UFP subchronic exposure induces Nrf2 activation and antioxidant enzymes expression in aorta. Animals were exposed to FA as control group, CP, FP, and UFP. Nrf2 protein levels in the cytosolic extracts were detected by Western blotting ((a), top) and nuclear extracts were utilized to electrophoretic mobility shift assays of Nrf2 DNA binding activity ((a), bottom). mRNA levels for antioxidant genes in aorta tissue were determined by RT-PCR for subchronic exposure ((b), (c), and (d)). Bottom images are representative from agarose gels. Densitometry analysis is expressed as mean ± SD ($n = 6$ animals per group). *indicates statistical differences ($p < 0.05$) respect FA. HO-1: heme oxigenase-1; SOD2, superoxide dismutase type-2; GST, glutathione S-transferase; RT-PCR: reverse transcriptase-polymerase chain reaction; FA: filtered air; CP: coarse particulate; FP: fine particulate; UFP: ultrafine particulate; Nrf2: nuclear factor erythroid-2.

PM induces DNA oxidative adducts such as 7-hydro-8-oxo-2′-deoxyguanosine (8-oxodG) in animal models,[40] and even when the PAH content is low in $PM_{2.5}$. After their metabolic activation by functional CYP1A1, PM can produce PAH–DNA bulky adducts, 8-oxodG, and DNA strand breaks in cell lines.[18] Sørensen et al. reported that $PM_{2.5}$ exposure was found to be a predictor of an increase in 8-oxodG in lymphocyte DNA in subjects exposed to it.[41] Further studies are needed to determine the type of DNA damage, the DNA repair mechanisms, and why UFP exposure induces permanent DNA adducts.

Lung Nrf2 response and antioxidant enzyme induction

Nrf2 activation is a key downstream regulatory factor of cell survival and sensitive markers in response to OxS.[12] The activation of Nrf2 in the lung of rats exposed to PM fractions shows that FP and UFP induced the activation of Nrf2 in the lung compared with the FA control group of cytosolic Nrf2 in the FP and UFP compared with FA group.

Our data are consistent with those reported by Li et al. and Baulig et al., who observed that after exposure to diesel exhaust particle (DEP), Nfr2 is activated and induces the mRNA expression of HO-1,[42] and Nrf2 binds to the ARE consensus sequence in the GST or NAD(P)H quinone dehydrogenase 1 (NQO1) promoter,[43] respectively.

The nuclear translocation of Nrf2 results in the gene transcription of antioxidants and phase-II defense enzymes, such as γ-GCS, NQO1, SOD2, GST, and HO-1, by binding to the ARE.[11] The mRNA levels of *HO-1*, *SOD2*, and *GST* genes were determined in this study as markers of the antioxidant defense against OxS induced by PM exposure. The induction response of these genes was observed after exposure to FP and UFP, although some differences in the response of each gene to the particulate fractions were observed; these results corroborate the published information on the induction of Nrf2 activity seen in FP and UFP groups in acute and subchronic exposure in different brain regions.[23]

The rapid induction of HO-1 increases the rate of free heme catabolism via the formation of carbon monoxide (CO) and biliverdin, and HO-1 confers cytoprotective effects through the biliverdin–bilirubin system.[44–46] The overexpression of HO-1 has cytoprotective effects in the lung, with a large beneficial spectrum of effects in several lung diseases.[47] The acute HO-1 mRNA induction observed in the UFP group suggests a cytoprotective effect to the smallest particulate fraction toxicity. Moreover, our results corroborate a previous study by Li et al. (2003), who observed an induction of HO-1 dependence on the particle size that could be related to the high organic content of UFP, and to the redox activity.[42] However, subchronic exposure to any PM fraction did not induce HO-1 mRNA expression, suggesting a secondary effect on the gene regulation of HO-1 or the nonparticipation of HO-1 in the chronic toxicity of the PM.

GST catalyzes the addition of reduced glutathione to electrophilic species and is important in the detoxification of the oxidizing agents that are produced due to a normal cellular activity.[48] GST-Pi, which corresponds to the sequence that we tested, is known to be involved in protein interaction (1-Cys peroxiredoxin) and related to the susceptibility to developing lung and esophageal cancer and other lung diseases such as asthma.[49,50] Our results imply the induction of GST-Pi by exposure to FP and UFP in a time-dependent response, which might be influenced by the particle size and chemical composition and could be involved in the development of lung diseases.

SOD2, also termed manganese superoxide dismutase, is the main antioxidant enzyme in the inner mitochondrial matrix that protects mitochondrial DNA and mitochondrial function, and it has been identified in cell senescence.[51,52] Exposure to PM, FP, and UFP has the mitochondria as a target organelle at a cellular level. Li et al. (2003) observed the presence of UFP, and to a lesser degree FP, into the mitochondria of murine macrophages and human bronchial epithelial cells.[42] In contrast, Hiura et al. (2000) reported that the organic chemicals extracted from DEP could induce a decrease in the mitochondrial membrane potential and intracellular ATP production in RAW 264.7 cells.[53] Our results indicate that SOD2 expression has been increased only in response to FP and UFP in acute and subchronic exposures suggesting an oxidative damage in mitochondria from lung tissue.

According to our results, the antioxidant response in the lung is influenced by the particle fraction, the exposure time, and Nrf2-target gene evaluated.

Lung inflammation response to PM fractions

Inhalation of PM caused inflammation of the airways and lungs (local inflammation), as one of the main toxic mechanisms of PM that could be responsible for secondary adverse effects on other tissues, for example, cardiovascular effects, or the development of systemic responses as reported by Mutlu et al.[54]

IL-1β, IL-6, and TNF-α participate in the production of various other pro-inflammatory cytokines and hepatic acute phase proteins. It has been suggested that TNF-α is a key player in the innate immune system in the cytokine network and in the activation and recruitment of inflammatory cells.[55] In the present study, we did not observe statistically significant differences in the TNF-α concentrations in BALF among the PM exposure groups. TNF-α could be downregulated during acute PM exposure by the IL-6 cytokine,[56,57] in agreement with the findings presented herein.

IL-1β is defined as a prototype pro-inflammatory and "alarm" cytokine. It is produced rapidly by macrophages in response to inflammatory stimuli, inducing different immune cellular and molecular mechanisms that include the expression and synthesis of adhesion molecules (e.g. ICAM-1 and VCAM-1) and nitric oxide. They promote the infiltration of inflammatory and immunocompetent cells from the circulation into extravascular space and tissues.[58] We observed the presence of IL-1β in BALF only after acute exposure to UFP, suggesting that this inflammatory response could be mediated by the presence of the smallest particulates, which have higher surface areas than do CP and FP. However, IL-1β production and TNF-α could be inhibited or modulated by IL-6.

We observed that IL-6 increased after acute exposure to FP and UFP. IL-6 production is sensitive to IL-1β; the high IL-6 concentration inhibited the production of IL-1β and TNF-α. Our results could explain the nonresponse of TNF-α concentrations in BALF in the same particulate groups and the unresponsiveness in IL-1β in the FP group. Additionally, IL-6 is involved in the hepatic induction of acute phase response inducing proteins related to restoring the disturbed homeostasis due to the immune process, such as fibrinogen,[59] which has been reported to increase after PM exposure.[60] This finding suggests that IL-6 release by PM exposure is related to a coagulation effect.[54]

IL-1β and IL-6 concentrations indicated an inflammatory response. To investigate the chemotaxis signal in the lung, we evaluated the concentration of the chemotactic molecule MIP-2, which is homologous to IL-8 in humans. An increment in MIP-2 concentration in BALF was observed in the acute exposure to FP and UFP; these results confirm the release of humoral mediators in the immune response against small particulates (<2.5 μm). MIP-2 is involved in the recruitment of neutrophils in the lungs and mediates the acute inflammatory response following exposure to particles.[15] Our results are consistent with other studies that used particles from different origins. It has been reported that exposure to higher doses of DEPs increased the expression level of *IL-6* and *MIP-2*, independent of *TNF-α* status in C57×CBA mice.[58]

Significant increments in IL-1β, IL-6, and MIP-2 after acute exposure could be due to OxS, the chemical composition (transition metals and PAH), or simply the

interaction of FP and UFP fractions with the alveolar macrophages.[60]

An important observation was the absence of cytokines in the BALF in the group exposed to the CP fraction. *In vitro* studies using PM_{10} as representative particles of CP suggested a pro-inflammatory response;[60] however, other factors could influence unresponsiveness to CP exposure such as: (1) the mucociliary clearance,[61] CP deposition in upper airways including the bronchial tree; and (2) anatomic features of the *in vivo* model, nasal turbinate bones, bearing sensory epithelium, confer additional surface area, and increase the air turbulence to enhance the air particulates deposition.[62] Differences in the turbinate dimension between species can influence the deposition of CP, *Rattus norvergicus*, for example, has long and deep turbinates compared to those of humans. For these reasons, possibly CP exposure did not induce antioxidant and immune responses in the rat model.

Our results for cytokines in BALF did not support the hypothesis of chronic inflammation during repeated exposures to PM. However, we cannot rule out that other cytokines such as IL-4, IL-10, and TGF-β, which can modulate immune cells and decrease inflammatory response and mediators, are induced in the subchronic response to PM. The immunological response to constant stimuli along a relatively large exposure period could modulate the immune response to protect from tissue damage and initiate the tissue remodeling. It has been observed that $PM_{2.5}$ and $PM_{10\text{-}2.5}$ exposure induced Toll-like-receptor expression and increased the pro-inflammatory cytokines in the early phase of the immune response.[63] Future studies are needed to confirm *in vivo* the immune response balance present during the chronic exposure to PM.

Nrf2 mediates antioxidant response in aorta

In epidemiological studies, exposure to FP and UFP has been associated with adverse health effects, including cardiorespiratory diseases.[64,65] Many hypotheses have been postulated to explain the mechanisms responsible for the adverse effects of FP exposure.[65,66] One of the most accepted hypotheses is that PM causes OxS in the airways and induces an inflammatory response with an upregulation of OxS-sensitive pathways. Moreover, FP and UFP can cross the epithelial alveolar-endothelium barrier, reach the pulmonary circulation, and be distributed into the heart, with direct interactions with the systemic vasculature generating adverse effects at various sites.[16,66,67] Several studies have assessed the direct effect of particles *in vivo*[68,69] and *ex vivo*.[70–73] However, studies to evaluate the effect of PM translocation are needed, since it is known that UFP can get across the alveolar-endothelium barrier.[4]

We propose that PM fractions can induce OxS in the aorta after their initial effect in the lung. Our study provides evidence that exposure to any PM fraction was not associated with Nrf2 activation or *SOD2*, *HO-1*, and *GST* expression in the aorta after an acute exposure. In contrast, we found that the antioxidant response occurred only after repeated exposures during subchronic exposure.

Similar effects have been found in other studies: a study in *ApoE*$^{-/-}$ mice showed that UFP induced OxS at early stages of atherosclerosis, inducing the mRNA liver expression of Nrf2-related genes. It is thought that the FP and UFP fractions have more long-term health effects but that the CP fraction is associated with short-term health effects.[74]

We demonstrated that the subchronic exposure to FP and UFP caused Nrf2 activation in the aorta. However, the subchronic exposure to CP resulted in a significant increase in the gene transcription of HO-1 mRNA in the aorta. Previously, we demonstrated that CP exposure induced the expression of components of the angiotensin endocrine system and that subchronic exposure to CP increased the intramyocardial coronary artery thickness. The HO-1 effect by CP in aorta might result in pulmonary and cardiac effects on angiotensin in these tissues through a different mechanism.[75]

The increased toxicity of UFP can be explained by their small size, large particle number per unit of mass, high organic carbon content, high content of PAHs, and ability to reach subcellular organelles, such as mitochondria.[7] OxS could be the central mechanism by which ambient PM induces adverse health effects. Moreover, the small size of UFP allows their access to the systemic circulation, and they can be involved in inflammatory events in the vessel wall, for example, atherosclerosis, or translocated from the lungs into the circulation and extrapulmonary organs (i.e. liver, heart, spleen, and brain).[4,66] Our study demonstrates that antioxidant enzymes in aorta were observed when Nrf2 is activated but only after subchronic exposure to FP and UFP.

Our study data correlate with those of Araujo et al., who found that exposure to FP and UFP in *ApoE*$^{-/-}$ mice led to increased hepatic lipoperoxidation, accompanied by a higher upregulation of Nrf2-regulated antioxidant genes and unfolded protein response genes of UFP-exposed mouse livers.[21]

Chemical composition is related to PM fraction effect

This is the first study to evaluate the time- and PM size-related induction of OxS, DNA damage, and inflammation in the lung and the effect on the aorta, which is not a direct target tissue described in PM toxicity.

Previously, we reported the particulate concentration measured in whole body chamber exposure and the chemical composition (transition metals and PAH) from the present exposure.[23] In addition, it has been reported that the CP and FP fractions from Mexico City contain metals such as Fe, Zn, and Ti and, to a lesser extent, Mn, Cu, V, Cd, Ni, Cr, and Pb. There are also high levels of organic and elemental carbon, endotoxins, and PAHs.[76] Transition and divalent metals exposure can explain the effect of the

different PM fractions on the deregulation of cardiovascular system control because these metals can impact allosteric sites or interfere with calcium pathways.[75] However, in the present study, we now demonstrate that the small fractions (<2.5 μm) can be involved in OxS induction via prooxidant activity promoting ROS production by divalent metals and a significant concentration of PAH.

PAHs are important in the toxicity of the UFP because PAH *in vitro* cell models demonstrate the expression of HO-1. Our results from carcinogen-DNA adducts, inflammation, and antioxidant Nrf2 response support the hypothesis of UFP as being more reactive. Although we did not determine the UFP mass and chemical composition, FP characterization, which includes the UFP fraction, indicated a high total concentration of PAH (10.1 $\mu g/m^3$) and CP (2.8 $\mu g/m^3$), which could explain the major effects observed in the present study.

Conclusions

The present study indicates that the exposure to PM induced OxS, DNA damage, and inflammation in the lung, which was dependent on the particle size and the time of exposure. Exposure to FP and UFP induced higher oxidative damage and Nrf2 antioxidant response in the lung than CP exposure did. The effect of FP and UFP on the antioxidant Nrf2-dependent response induction is mainly evident in the subchronic exposure in the aorta. We concluded that UFP is the main particulate fraction related to OxS, DNA damage, and inflammation in the lung, mainly as an acute response. DNA damage persisted in the subchronic exposure. Additionally, an effective response of Nrf2 antioxidant-related elements in the aorta as a representative of systemic vasculature was observed in the subchronic exposure. We observed the biological plausibility of OxS translocated from the lung to the vascular system after repeated exposure.

Declaration of conflicting interests

The author(s) declared no potential conflicts of interest with respect to the research, authorship, and/or publication of this article.

Funding

The author(s) disclosed receipt of the following financial support for the research, authorship, and/or publication of this article: This work was financially supported by Consejo Nacional de Ciencia y Tecnología (167778 and 57752) and NIH Fogarty Grant (5D43TW000623).

ORCID iD

A Osornio-Vargas http://orcid.org/0000-0001-8287-7102
A De Vizcaya-Ruiz http://orcid.org/0000-0002-2097-0464

References

1. Pope CA, Burnett RT, Thun MJ, et al. Lung cancer, cardiopulmonary mortality, and long-term exposure to fine particulate air pollution. *JAMA* 2002; **287**(9): 1132–1141.
2. Lin CC, Chen SJ, Huang KL, et al. Characteristics of metals in nano/ultrafine/fine/coarse particles collected beside a heavily trafficked road. *Environ Sci Technol* 2005; **39**(21): 8113–8122.
3. Happo MS, Salonen RO, Hälinen AI, et al. Dose and time dependency of inflammatory responses in the mouse lung to urban air coarse, fine, and ultrafine particles from six European cities. *Inhal Toxicol* 2007; **19**(3): 227–246.
4. Oberdörster G, Oberdörster E and Oberdörster J. Nanotoxicology: an emerging discipline evolving from studies of ultrafine particles. *Environ Health Perspect* 2005; **113**(7): 823–839.
5. Wallenborn JG, Schladweiler MJ, Richards JH, et al. Differential pulmonary and cardiac effects of pulmonary exposure to a panel of particulate matter-associated metals. *Toxicol Appl Pharmacol* 2009; **241**(1): 71–80.
6. Rubio V, Valverde M and Rojas E. Effects of atmospheric pollutants on the Nrf2 survival pathway. *Environ Sci Pollut Res Int* 2010; **17**(2): 369–382.
7. Li N, Sioutas C, Cho A, et al. Ultrafine particulate pollutants induce oxidative stress and mitochondrial damage. *Environ Health Perspect* 2003; **111**(4): 455–460.
8. Hur W and Gray NS. Small molecule modulators of antioxidant response pathway. *Curr Opin Chem Biol* 2011; **15**(1): 162–173.
9. Rangasamy T, Cho CY, Thimmulappa RK, et al. Genetic ablation of Nrf2 enhances susceptibility to cigarette smoke-induced emphysema in mice. *J Clin Invest* 2004; **114**(9): 1248–1259.
10. Papaiahgari S, Yerrapureddy A, Reddy SR, et al. Genetic and pharmacologic evidence links oxidative stress to ventilator-induced lung injury in mice. *Am J Respir Crit Care Med* 2007; **176**(12): 1222.
11. Cho HY and Kleeberger SR. Nrf2 protects against airway disorders. *Toxicol Appl Pharmacol* 2010; **244**(1): 43–56.
12. Kensler TW, Wakabayashi N and Biswal S. Cell survival responses to environmental stresses via the keap1-Nrf2-ARE pathway. *Annu Rev Pharmacol Toxicol* 2007; **47**(1): 89–116.
13. Kaspar JW, Niture SK and Jaiswal AK. Nrf2: INrf2 (Keap1) signaling in oxidative stress. *Free Radic Biol Med* 2009; **47**(9): 1304–1309.
14. Araujo JAA. Particulate air pollution, systemic oxidative stress, inflammation, and atherosclerosis. *Air Qual Atmos Heal* 2011; **4**(1): 79–93.
15. Driscoll KE. TNFα and MIP-2: role in particle-induced inflammation and regulation by oxidative stress. *Toxicol Lett* 2000; **112**: 177–183.
16. Mills NL, Donaldson K, Hadoke PW, et al. Adverse cardiovascular effects of air pollution. *Nat Clin Pr Cardiovasc Med* 2009; **6**(1): 36–44.

17. Danielsen PH, Loft S, Jacobsen NR, et al. Oxidative stress, inflammation, and DNA damage in rats after intratracheal instillation or oral exposure to ambient air and wood smoke particulate matter. *Toxicol Sci* 2010; **118**(2): 574–585.
18. Abbas I, Garçon G, Saint-Georges F, et al. Polycyclic aromatic hydrocarbons within airborne particulate matter (PM2. 5) produced DNA bulky stable adducts in a human lung cell coculture model. *J Appl Toxicol* 2013; **33**(2): 109–119.
19. Rossner P, Topinka J, Hovorka J, et al. An acellular assay to assess the genotoxicity of complex mixtures of organic pollutants bound on size segregated aerosol. Part II: oxidative damage to DNA. *Toxicol Lett* 2010; **198**(3): 312–316.
20. Ntziachristos L, Froines JR, Cho AK, et al. Relationship between redox activity and chemical speciation of size-fractionated particulate matter. *Part Fibre Toxicol* 2007; **4**(1): 5.
21. Araujo JA, Barajas B, Kleinman M, et al. Ambient particulate pollutants in the ultrafine range promote early atherosclerosis and systemic oxidative stress. *Circ Res* 2008; **102**(5): 589–596.
22. Kim S, Jaques PA, Chang M, et al. Versatile aerosol concentration enrichment system (VACES) for simultaneous in vivo and in vitro evaluation of toxic effects of ultrafine, fine and coarse ambient particles. Part II: field evaluation. *J Aerosol Sci* 2001; **32**(11): 1299–1314.
23. Guerra R, Vera-Aguilar E, Uribe-Ramirez M, et al. Exposure to inhaled particulate matter activates early markers of oxidative stress, inflammation and unfolded protein response in rat striatum. *Toxicol Lett* 2013; **222**(2): 146–154.
24. Phillips DH and Arlt VM. The 32P-postlabeling assay for DNA adducts. *Nat Protoc* 2007; **2**(11): 2772–2781.
25. Valdés-Arzate A, Luna A, Bucio L, et al. Hepatocyte growth factor protects hepatocytes against oxidative injury induced by ethanol metabolism. *Free Radic Biol Med* 2009; **47**(4): 424–430.
26. Bradford MM. A rapid and sensitive method for the quantitation of microgram quantities of protein using the principle of protein dye binding. *Anal Biochem* 1976; **72**: 248–254.
27. Marnett LJ. Oxyradicals and DNA damage. *Carcinogenesis* 2000; **21**(3): 361–370.
28. Peters A, Wichmann HE, Tuch T, et al. Respiratory effects are associated with the number of ultrafine particles. *Am J Respir Crit Care Med* 1997; **155**(4): 1376–1383.
29. Brunekreef B and Holgate ST. Air pollution and health. *Lancet* 2002; **360**(9341): 1233–1242.
30. Osburn WO and Kensler TW. Nrf2 signaling: an adaptive response pathway for protection against environmental toxic insults. *Mutat Res Rev Mutat Res* 2008; **659**(1-2): 31–39.
31. Donaldson K, Brown D, Clouter A, et al. The pulmonary toxicology of ultrafine particles. *J Aerosol Med* 2002; **15**(2): 213–220.
32. Li N, Hao M, Phalen RF, et al. Particulate air pollutants and asthma. A paradigm for the role of oxidative stress in PM-induced adverse health effects. *Clin Immunol* 2003; **109**(3): 250–265.
33. Zhang W, Cao YX, He JY, et al. Down-regulation of α1-adrenoceptor expression by lipid-soluble smoke particles through transcriptional factor nuclear factor-κB pathway. *Basic Clin Pharmacol Toxicol* 2007; **101**(6): 401–406.
34. Dalle-Donne I, Giustarini D, Colombo R, et al. Protein carbonylation in human diseases. *Trends Mol Med* 2003; **9**(4): 169–176.
35. Dalle-Donne I, Aldini G, Carini M, et al. Protein carbonylation, cellular dysfunction, and disease progression. *J Cell Mol Med* 2006; **10**(2): 389–406.
36. Suzuki YJ, Carini M and Butterfield DA. Protein carbonylation. *Antioxid Redox Signal* 2010; **12**(3): 323–325.
37. Nyström T. Role of oxidative carbonylation in protein quality control and senescence. *EMBO J* 2005; **24**(7): 1311–1317.
38. Curtis JM, Hahn WS, Long EK, et al. Protein carbonylation and metabolic control systems. *Trends Endocrinol Metab* 2012; **23**(8): 399–406.
39. Giustarini D, Rossi R, Milzani A, et al. S-glutathionylation: from redox regulation of protein functions to human diseases. *J Cell Mol Med* 2004; **8**(2): 201–212.
40. Møller P, Jacobsen NR, Folkmann JK, et al. Role of oxidative damage in toxicity of particulates. *Free Radic Res* 2010; **44**(1): 1–46.
41. Sørensen M, Autrup H, Møller P, et al. Linking exposure to environmental pollutants with biological effects. *Mutat Res Mutat Res* 2003; **544**(2–3): 255–271.
42. Li N, Venkatesan MI, Miguel A, et al. Induction of heme oxygenase-1 expression in macrophages by diesel exhaust particle chemicals and quinones via the antioxidant-responsive element. *J Immunol* 2000; **165**(6): 3393–3401.
43. Baulig A, Sourdeval M, Meyer M, et al. Biological effects of atmospheric particles on human bronchial epithelial cells. Comparison with diesel exhaust particles. *Toxicol In Vitro* 2003; **17**(5–6): 567–573.
44. Ryter SW, Otterbein LE, Morse D, et al. Heme oxygenase/carbon monoxide signaling pathways: regulation and functional significance. *Mol Cell Biochem* 2002; **234–235**(1–2): 249–263.
45. Otterbein LE and Choi AM. Heme oxygenase: colors of defense against cellular stress. *Am J Physiol Lung Cell Mol Physiol* 2000; **279**(6): 1029–1037.
46. Shibahara S. The heme oxygenase dilemma in cellular homeostasis: new insights for the feedback regulation of heme catabolism. *Tohoku J Exp Med* 2003; **200**(4): 167–186.
47. Fredenburgh LE, Perrella MA and Mitsialis SA. The role of heme oxygenase-1 in pulmonary disease. *Am J Respir Cell Mol Biol* 2007; **36**(2): 158–165.
48. Sherratt PJ and Hayes JD. Glutathione S-transferases. In: Ioannides C (ed) *Enzyme systems that metabolise drugs and other xenobiotics [Internet]*. Chichester: John Wiley & Sons, Ltd, 2002, pp. 319–352.
49. Vasieva O. The many faces of glutathione transferase pi. *Curr Mol Med* 2011; **11**(2): 129–139.
50. Conklin DJ, Haberzettl P, Prough RA, et al. Glutathione-S-transferase P protects against endothelial dysfunction induced

by exposure to tobacco smoke. *Am J Physiol Hear Circ Physiol* 2009; **296**(5): H1586–H1597.
51. Wegesser TC, Franzi LM, Mitloehner FM, et al. Lung antioxidant and cytokine responses to coarse and fine particulate matter from the great California wildfires of 2008. *Inhal Toxicol* 2010; **22**(7): 561–570.
52. Zelko IN, Mariani TJ and Folz RJ. Superoxide dismutase multigene family: a comparison of the CuZn-SOD (SOD1), Mn-SOD (SOD2), and EC-SOD (SOD3) gene structures, evolution, and expression. *Free Radic Biol Med* 2002; **33**(3): 337–349.
53. Hiura TS, Li N, Kaplan R, et al. The role of a mitochondrial pathway in the induction of apoptosis by chemicals extracted from diesel exhaust particles. *J Immunol* 2000; **165**(5): 2703–2711.
54. Mutlu GM, Green D, Bellmeyer A, et al. Ambient particulate matter accelerates coagulation via an IL-6-dependent pathway. *J Clin Invest* 2007; **117**(10): 2952–2961.
55. Wajant H, Pfizenmaier K and Scheurich P. Tumor necrosis factor signaling. *Cell Death Differ* 2003; **10** (1350–9047 (Print)): 45–65.
56. Aderka D, Le JM and Vilcek J. IL-6 inhibits lipopolysaccharide-induced tumor necrosis factor production in cultured human monocytes, U937 cells, and in mice. *J Immunol* 1989; **143**(11): 3517–3523.
57. Ulich TR, Yin S, Guo K, et al. Intratracheal injection of endotoxin and cytokines. II. Interleukin-6 and transforming growth factor beta inhibit acute inflammation. *Am J Pathol* 1991; **138**(5): 1097–1101.
58. Saber AT, Jacobsen NR, Bornholdt J, et al. Cytokine expression in mice exposed to diesel exhaust particles by inhalation. Role of tumor necrosis factor. *Part Fibre Toxicol* 2006; **3**: 4.
59. Heinrich PC, Castell JV and and Andus T. Interleukin-6 and the acute phase response. *Biochem J* 1990; **265**(3)**:** 621–636.
60. Osornio-Vargas ÁR, Bonner JC, Alfaro-Moreno E, et al. Proinflammatory and cytotoxic effects of Mexico City air pollution particulate matter in vitro are dependent on particle size and composition. *Environ Health Perspect* 2003; **111**(10): 1289–1293.
61. Stuart BO. Deposition and clearance of inhaled particles. *Environl Health Perspect* 1976; **16**: 41–53.
62. Hillenius WJ. The evolution of nasal turbinates and mammalian endothermy. *Paleobiology* 1992; **18**(1): 17–29.
63. Miyata R and van Eeden SF. The innate and adaptive immune response induced by alveolar macrophages exposed to ambient particulate matter. *Toxicol Appl Pharmacol*. 2011; **257**(2): 209–226.
64. Pope CA and Dockery DW. Health effects of fine particulate air pollution: lines that connect. *J Air Waste Manage Assoc* 2006; **56**(6): 709–742.
65. Atkinson RW, Anderson HR, Sunyer J, et al. Acute effects of particulate air pollution on respiratory admissions: results from APHEA 2 project. *Am J Respir Crit Care Med* 2001; **164**(10 I): 1860–1866.
66. Nemmar A, Hoylaerts MF, Hoet PHM, et al. Possible mechanisms of the cardiovascular effects of inhaled particles: systemic translocation and prothrombotic effects. *Toxicol Lett* 2004; **49**(1–3): 243–253.
67. Vermylen J, Nemmar A, Nemery B, et al. Ambient air pollution and acute myocardial infarction. *J Thromb Haemost [Internet]* 2005; **3**(9): 1955–1961.
68. Da Silva DR, Binotti RS, Da Silva CM, et al. Mites in dust samples from mattress surfaces from single beds or cribs in the south Brazilian city of Londrina. *Pediatr Allergy Immunol* 2005; **16**(2): 132–136.
69. Nemmar A and Inuwa IM. Diesel exhaust particles in blood trigger systemic and pulmonary morphological alterations. *Toxicol Lett* 2008; **176**(1): 20–30.
70. Meiring JJ, Borm PJA, Bagate K, et al. The influence of hydrogen peroxide and histamine on lung permeability and translocation of iridium nanoparticles in the isolated perfused rat lung. *Part Fibre Toxicol* 2005; **2**: 3.
71. Hamoir J, Nemmar A, Halloy D, et al. Effect of polystyrene particles on lung microvascular permeability in isolated perfused rabbit lungs: role of size and surface properties. *Toxicol Appl Pharmacol* 2003; **190**(3): 278–285.
72. Nemmar A, Hamoir J, Nemery B, et al. Evaluation of particle translocation across the alveolo-capillary barrier in isolated perfused rabbit lung model. *Toxicology* 2005; **208**(1): 105–113.
73. Alfaro-Moreno E, Nawrot TS, Vanaudenaerde BM, et al. Co-cultures of multiple cell types mimic pulmonary cell communication in response to urban PM10. *Eur Respir J* 2008; **32**(5): 1184–1194.
74. Brunekreef B and Forsberg B. Epidemiological evidence of effects of coarse airborne particles on health. *Eur Respir J* 2005; **26**(2): 309–318.
75. Aztatzi-Aguilar OG, Uribe-Ramírez M, Arias-Montaño JA, et al. Acute and subchronic exposure to air particulate matter induces expression of angiotensin and bradykinin-related genes in the lungs and heart: angiotensin-II type-I receptor as a molecular target of particulate matter exposure. *Part Fibre Toxicol* 2015; **12**(1): 17.
76. De Vizcaya-Ruiz A, Gutiérrez-Castillo ME, Uribe-Ramirez M, et al. Characterization and in vitro biological effects of concentrated particulate matter from Mexico City. *Atmos Environ* 2006; **40**: 583–592.